JOC The Journal of Organic Chemistry

Article

pubs.acs.org/joc

Factors Controlling the Reactivity and Selectivity of the Diels–Alder Reactions Involving 1,2-Azaborines

Yago García-Rodeja and Israel Fernández*

Departamento de Química Orgánica I, Facultad de Ciencias Químicas, Universidad Complutense, 28040 Madrid, Spain

Supporting Information

ABSTRACT: The factors controlling the reactivity and endo/exo selectivity of the Diels–Alder reactions involving 1,2-azaborines have been computationally explored within the density functional theory framework. It is found that the $AlCl_3$-catalyzed [4 + 2]-cycloaddition reaction between these dienes and *N*-methylmaleimide proceeds concertedly and leads almost exclusively to the corresponding endo cycloadduct, which is in good agreement with previous experimental observations. In addition, the effect of the substituent directly attached to the boron atom of the 1,2-azaborine on the process is also analyzed in detail. To this end, the combination of the activation strain model of reactivity and the energy decomposition analysis methods has been applied to gain a quantitative understanding into the origins of the endo selectivity of the process as well as the influence of the boron and nitrogen substituent on the barrier heights of the transformations.

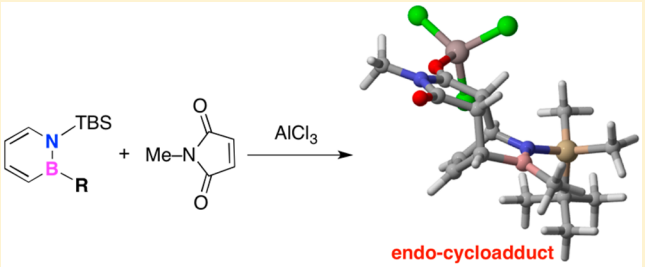

INTRODUCTION

The Diels–Alder reaction constitutes one of the most useful methodologies in organic synthesis due to its ability to increase molecular complexity in a single synthetic step.[1,2] Indeed, this [4 + 2]-cycloaddition reaction can potentially set up to four stereocenters in a regioselective and stereospecific manner, and for this reason, it is not surprising that this process has been widely applied toward the synthesis of a great number of target molecules including complex natural products.[3,4] One important feature shared by many Diels–Alder reactions is that they predominantly lead to the formation of the corresponding endo cycloadduct, particularly when using rigid dienophiles such as maleic anhydride or benzoquinone. The origin of this preference, known as the Alder rule,[5] is still controversial in view of the different arguments used to explain the observed stereocontrol. Among them, inductive effects,[6] charge-transfer,[7] and CH···π interactions[8] or the occurrence of secondary orbital interactions[9] (SOI, initially proposed by Woodward and Hoffmann)[10] should be highlighted.

In this sense, the Diels–Alder reactions involving 1,2-azaborines and different dienophiles have been described very recently.[11] These particular dienes, isoelectronic and isostructural analogues of benzene where one CC bond is replaced by a BN bond, are attracting nowadays considerable interest in fields such as materials chemistry[12] or as pharmaceutical candidates[13] due to their peculiar electronic structure that is remarkably different from that of benzene. Thus, Liu and co-workers found that *N*-TBS-B-Me-1,2-azaborine (TBS = *tert*-butyldimethylsilyl) undergoes irreversible Diels–Alder reactions with electron-deficient dienophiles in the presence of 20 mol % of $AlCl_3$ leading to the corresponding cycloadducts with almost complete endo diastereoselectivity (dr > 95:5, Scheme 1).[11]

Scheme 1. Diels–Alder Reaction between 1,2-Azaborines and Maleic Anhydride or *N*-Methylmaleimide Described by Liu and Co-workers (see reference 11)

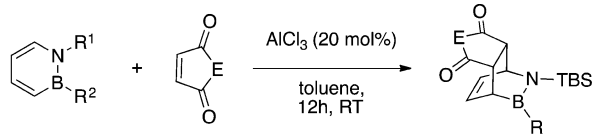

R^1 = TBS, R^2 = Me	E = O	96% (> 95:5 d.r.)
R^1 = TBS, R^2 = Me	E = N-Me	95% (> 95:5 d.r.)
R^1 = TBS, R^2 = ≡–H	E = O	< 5%
R^1 = TBS, R^2 = H	E = O	< 5%
R^1 = Boc, R^2 = Me	E = O	< 5%

In contrast, it was observed that the analogous sp-hybridized B-alkynyl or B–H-substituted 1,2-azaborines practically did not produce the expected cycloadducts (reaction yields lower than 5%, Scheme 1) under similar reaction conditions. Although this difference in reactivity has been initially ascribed to the aromaticity strength of the initial 1,2-azaborine,[11] the physical factors controlling both the Diels–Alder reactivity and the endo selectivity of the process involving these dienes are not completely understood so far.

For this reason, herein we decided to apply the combination of the so-called activation strain model (ASM)[14] of reactivity and the energy decomposition analysis (EDA)[15] methods to gain quantitative insight into the Diels–Alder reactions involving these 1,2-azaborines. This ASM–EDA approach has successfully contributed to our current understanding of

Received: May 19, 2016
Published: July 6, 2016

DOI: 10.1021/acs.joc.6b01182
J. Org. Chem. 2016, 81, 6554–6562

different types of fundamental processes in organic chemistry (such as S_N2 and E2 reactions[16] and pericyclic reactions[17]) as well as metal-promoted transformations.[18] Interestingly, the ASM−EDA method has been particularly helpful to rationalize the regioselectivity of the Diels−Alder reactions involving fullerenes and related species[19] and to provide an alternative explanation for the endo selectivity of the textbook Diels−Alder reaction between maleic anhydride and cyclopentadiene.[20] Therefore, herein we report the application of the ASM−EDA method to the Diels−Alder reactions between 1,2-azaborines **1a−d** and *N*-methylmaleimide (Scheme 2). Issues such as the

Scheme 2. Diels−Alder Reactions between 1,2-Azaborines 1a−d and *N*-Methylmaleimide Considered in This Study

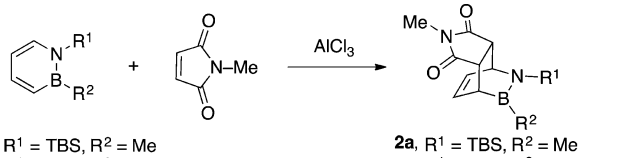

1a, R^1 = TBS, R^2 = Me
1b, R^1 = TBS, R^2 = H
1c, R^1 = TBS, R^2 = ≡—H
1d, R^1 = CO_2Me, R^2 = Me

2a, R^1 = TBS, R^2 = Me
2b, R^1 = TBS, R^2 = H
2c, R^1 = TBS, R^2 = ≡—H
2d, R^1 = CO_2Me, R^2 = Me

observed reactivity trend and regioselectivity as well as the influence of the aromaticity of the initial azaborine and the corresponding transition structures on the transformation will be analyzed in detail.

THEORETICAL METHODS

Computational Details. All the calculations reported in this paper were obtained with the Gaussian 09 suite of programs.[21] All reactants, transition structures, and cycloadducts were optimized using the B3LYP functional[22] in conjunction with the D3 dispersion correction suggested by Grimme et al.[23] using the double-ζ quality def2-SVP basis sets[24] for all atoms. Solvents effects were taken into account during the geometry optimizations using the polarizable continuum model (PCM).[25] All stationary points were characterized by frequency calculations.[26] Reactants and cycloadducts have positive definite Hessian matrices, whereas transition structures (TS's) show only one negative eigenvalue in their diagonalized force constant matrices, and their associated eigenvectors were confirmed to correspond to the motion along the reaction coordinate under consideration using the intrinsic reaction coordinate (IRC) method.[27] Single point calculations at the B3LYP-D3 level using the triple-ζ quality plus polarization def2-TZVP basis set[24] for all atoms were performed on the optimized geometries to refine the computed energies. This level is denoted PCM(toluene)-B3LYP-D3/def2-TZVP//PCM(toluene)-B3LYP-D3/def2-SVP.

The aromatic character of the 1,2-azaborines and the corresponding transition structures has been assessed by computing the nucleus independent chemical shift (NICS)[28] values at the [3+1] ring critical point of the electron density.[29] This point was selected due its high sensitivity to diamagnetic effects and its unambiguous character.[30] These calculations have been carried out using the gauge invariant atomic orbital (GIAO) method[31] at the B3LYP/def2-SVP level using the geometries optimized at the PCM(toluene)-B3LYP-D3/def2-SVP level.

Activation Strain Analyses of Reaction Profiles. The introduction of the so-called *activation strain model* has allowed us to gain more insight into the physical factors which control how the activation barriers arise in different fundamental processes.[14] This method is also known as distortion/interaction model, as proposed by Houk and co-workers.[32] The activation strain model is a fragment approach to understanding chemical reactions, in which the height of reaction barriers is described and understood in terms of the original reactants. Thus, the potential energy surface $\Delta E(\zeta)$ is decomposed, along the reaction coordinate ξ, into the strain $\Delta E_{strain}(\zeta)$ associated with deforming the individual reactants plus the actual interaction $\Delta E_{int}(\zeta)$ between the deformed reactants (eq 1):

$$\Delta E(\zeta) = \Delta E_{strain}(\zeta) + \Delta E_{int}(\zeta) \quad (1)$$

Herein, the reaction coordinate is defined as the projection of the IRC on the forming C···C distance between the carbon atom of the 1,2-azaborine and the carbon atom of *N*-methylmaleimide. This reaction coordinate ζ undergoes a well-defined change in the course of the reaction from ∞ to the equilibrium C···C distance in the corresponding transition structures. Because most of the located concerted TSs are asynchronous, we considered in all cases the shortest C···C distance as the reaction coordinate.

The strain $\Delta E_{strain}(\zeta)$ is determined by the rigidity of the reactants and on the extent to which groups must reorganize in a particular reaction mechanism, whereas the interaction $\Delta E_{int}(\zeta)$ between the reactants depends on their electronic structure and on how they are mutually oriented as they approach each other. It is the interplay between $\Delta E_{strain}(\zeta)$ and $\Delta E_{int}(\zeta)$ that determines if and at which point along ζ a barrier arises. The activation energy of a reaction $\Delta E^{\ddagger} = \Delta E(\zeta^{TS})$ consists of the activation strain $\Delta E^{\ddagger}_{strain} = \Delta E_{strain}(\zeta^{TS})$ plus the TS interaction $\Delta E^{\ddagger}_{int} = \Delta E_{int}(\zeta^{TS})$ (eq 2):

$$\Delta E^{\ddagger} = \Delta E^{\ddagger}_{strain} + \Delta E^{\ddagger}_{int} \quad (2)$$

Furthermore, the interaction energy can be further decomposed by means of the so-called energy decomposition analysis (EDA)[15] method into the following meaningful terms (eq 3):

$$\Delta E_{int}(\zeta) = \Delta V_{elstat} + \Delta E_{Pauli} + \Delta E_{orb} + \Delta E_{disp} \quad (3)$$

The term ΔV_{elstat} corresponds to the classical electrostatic interaction between the unperturbed charge distributions of the deformed reactants and is usually attractive. The Pauli repulsion ΔE_{Pauli} comprises the destabilizing interactions between occupied orbitals and is responsible for any steric repulsion. The orbital interaction ΔE_{orb} accounts for charge transfer (interaction between occupied orbitals on one moiety with unoccupied orbitals on the other, including HOMO−LUMO interactions) and polarization (empty-occupied orbital mixing on one fragment due to the presence of another fragment). Finally, the ΔE_{disp} term takes into account the interactions which are due to dispersion forces. The EDA calculations reported herein were carried out at the dispersion corrected BP86[33]-D3[23]/TZ2P[34] level using the optimized PCM-(toluene)-B3LYP-D3/def2-SVP geometries with the ADF 2014 program package.[35] This level is therefore denoted BP86-D3/TZ2P//PCM(toluene)-B3LYP-D3/def2-SVP.

RESULTS AND DISCUSSION

The [4 + 2]-cycloaddition reaction between *N*-TBS-B-Me-1,2-azaborine **1a** and *N*-methylmaleimide in the presence of $AlCl_3$

DOI: 10.1021/acs.joc.6b01182
J. Org. Chem. 2016, 81, 6554−6562

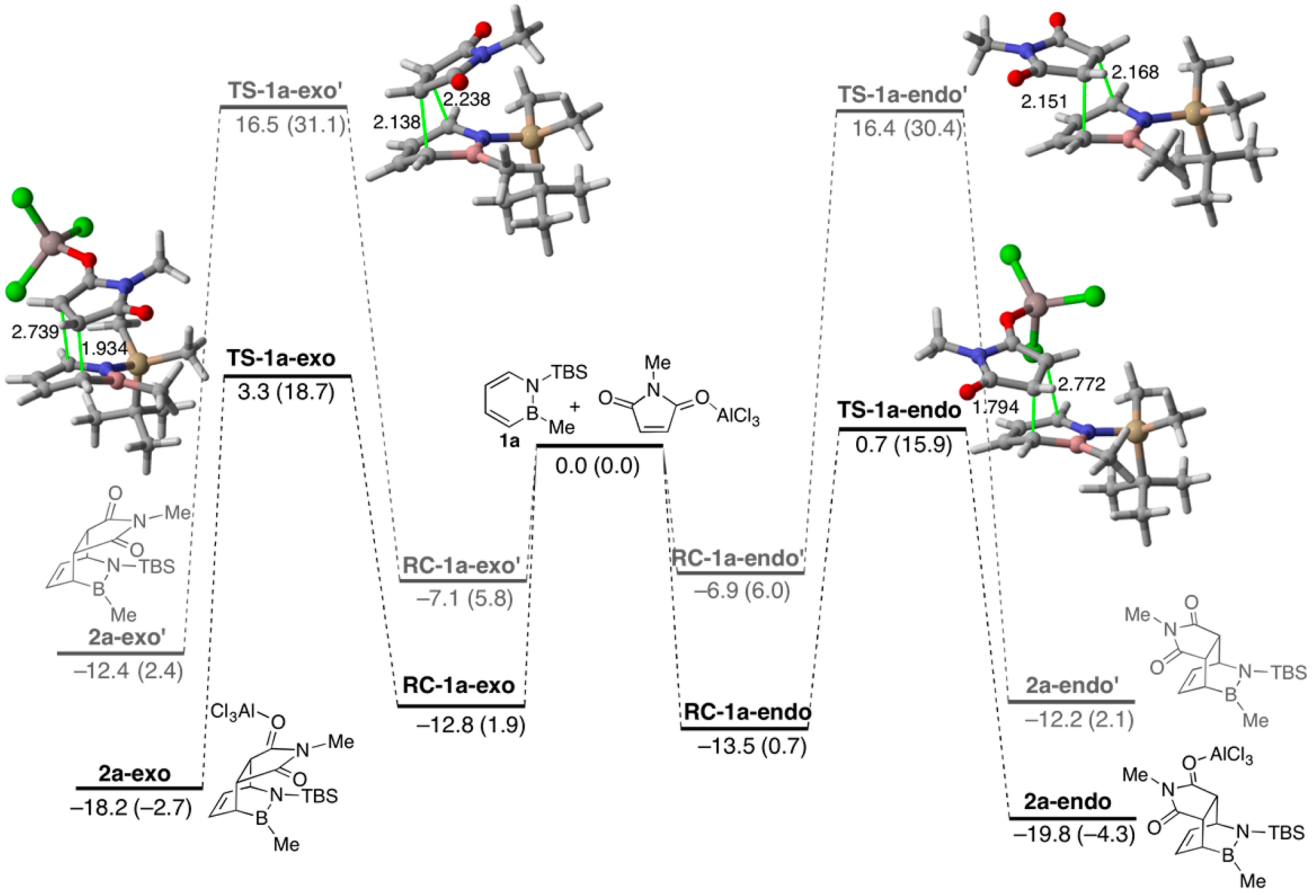

Figure 1. Computed reaction profiles for the uncatalyzed and $AlCl_3$-catalyzed Diels–Alder reactions between *N*-methylmaleimide and 1,2-azaborine **1a**. Relative energies (ZPVE included) and free energies (computed at 298 K, within parentheses) are given in kcal/mol whereas bond lengths are given in angstroms. All data have been computed at the PCM-(toluene)-B3LYP-D3/def2-TZVP//PCM(toluene)B3LYP-D3/def2-SVP level.

as catalyst was studied first. As readily seen in Figure 1, the process proceeds concertedly and leads to the formation of the thermodynamically more stable endo cycloadduct **2a-endo**.[36] The regioselectivity takes place under both kinetic and thermodynamic control, in view of the higher activation energy ($\Delta\Delta E^{\ddagger}$ = 2.6 kcal/mol) and less exothermic reaction energy ($\Delta\Delta E_R$ = 1.6 kcal/mol) computed for the formation of the corresponding exo cycloadduct **2a-exo**. Our calculated free activation energy difference ($\Delta\Delta G^{\ddagger}_{298}$ = 2.8 kcal/mol, measured at 298 K from the initial reactants) is consistent with the experimentally observed >95:5 endo:exo selectivity (see above).[11] This result together with the computed low activation barriers (<20 kcal/mol) and exothermicity, which are compatible with a process occurring at room temperature, support the selected computational methodology for the present study.

From the data in Figure 1, it becomes clear that the endo reaction pathway is favored along the entire reaction coordinate. Thus, not only are the corresponding transition state **TS-1a-endo** and the cycloadduct **2a-endo** more stable than **TS-1a-exo** and **2a-exo**, respectively, but also the initial reactant complex **RC-1a-endo** lies 0.7 kcal/mol below **RC-1a-exo**. Furthermore, inspection of the geometries of the transition states indicates that both saddle points are highly asynchronous, i.e., the C···C forming distances are not equivalent. This contrasts with the analogous transition state **TS-1a-endo′** computed for the uncatalyzed process where both C···C forming distances are nearly identical (see Figure 1). The latter saddle point lies 15.7 kcal/mol above the $AlCl_3$-counterpart, which confirms the activating effect of the $AlCl_3$ catalyst in the transformation. Indeed, it was experimentally observed that when the reaction between **1a** and maleic anhydride is carried out without Lewis acid, it requires 3 days at 110 °C to completion, which is consistent with our rather different computed activation energies for the processes involving **TS-1a-endo** and **TS-1a-endo′**. Finally, note that only the pathways where $AlCl_3$ is coordinated to the carbonyl group of *N*-methylmaleide oriented toward the *N*-TBS group are shown in Figure 1. We also computed the corresponding profiles where $AlCl_3$ is coordinated to the other carbonyl group of the dienophile and found that these alternative pathways are systematically higher in energy than those presented in Figure 1 (see Figure S1 in the Supporting Information).

The activation strain model (ASM) of reactivity was applied next to gain more quantitative insight into the physical factors controlling the barrier heights of the endo and exo cycloaddition pathways. Figure 2 shows the computed activation strain diagrams (ASD) for both approaches from the initial stages of the processes up to the corresponding transition states. As readily seen in Figure 2, both pathways exhibit quite similar ASD. Thus, in both cases the interaction energy between the deformed reactants, measured by the ΔE_{int} term, remains constant or becomes slightly destabilizing at the beginning of the reaction due to the onset of overlap and Pauli repulsion between the occupied π orbitals on either of the reactants. Despite that, the ΔE_{int} term inverts at a certain point

DOI: 10.1021/acs.joc.6b01182
J. Org. Chem. 2016, 81, 6554–6562

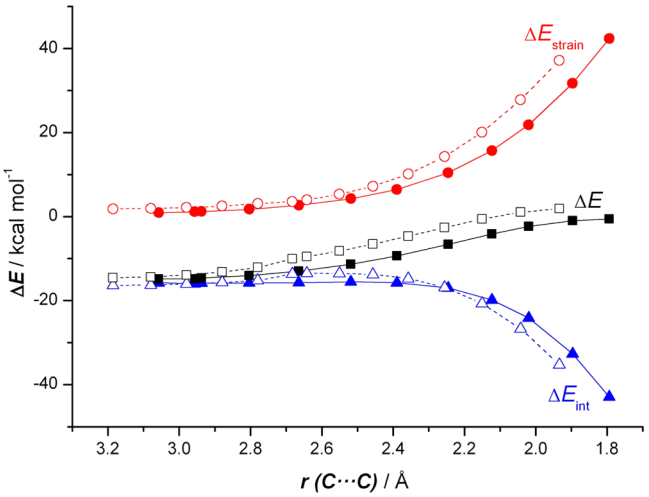

Figure 2. Comparative activation−strain diagrams for the endo (solid lines) and exo (dashed lines) approaches of the $AlCl_3$-catalyzed Diels−Alder reactions between *N*-methylmaleimide and 1,2-azaborine **1a** along the reaction coordinate projected onto the forming C···C bond distance. All data have been computed at the PCM(toluene)-B3LYP-D3/def2-TZVP//PCM(toluene)-B3LYP-D3/def2-SVP level.

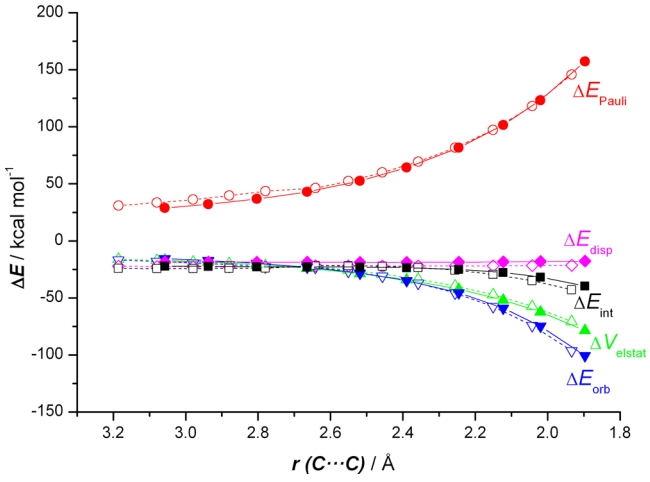

Figure 3. Decomposition of the interaction energy for the endo (solid lines) and exo (dashed lines) approaches of the $AlCl_3$-catalyzed [4 + 2]-cycloaddition reactions between *N*-methylmaleimide and 1,2-azaborine **1a** along the reaction coordinate projected onto the forming C···C bond distance. All data have been computed at the BP86-D3/TZ2P//PCM(toluene)-B3LYP-D3/def2-SVP level. Energies are given in kcal/mol and bond distances in angstroms.

along the reaction coordinate (i.e., at forming C···C distances of ca. 2.3−2.5 Å) and becomes more and more stabilizing as one approaches the corresponding transition state region. This behavior resembles that found not only for related Diels−Alder reactions[19,20] but also for other pericyclic reactions such as double-group transfer reactions[17a,c,g] or ene-ene-yne cyclizations.[17f] However, the stabilization provided by the interaction term cannot compensate for the strong destabilizing effect of the deformation energy required to adopt the transition state geometry (ΔE_{strain}), which therefore becomes the major factor controlling the activation barrier of the process.

The comparison between the endo- and exo-ASD clearly suggests that, contrary to the traditional view, the interaction energy between the deformed reactants is not at all decisive for the observed endo selectivity. Indeed, at the proximity of the corresponding transition state, the interaction along the exo pathway is even slightly more stabilizing than that along the endo pathway (see Figure 2). For instance, at the same C···C forming distance of 2.1 Å, a value of ΔE_{int} = −20.8 kcal/mol was computed for the endo pathway whereas a similar yet slightly lower (i.e., more stabilizing) value of ΔE_{int} = −23.6 kcal/mol was computed for the exo pathway (Figure 1). The rather similar interaction between the reactants along the reaction coordinate for both approaches is confirmed also in the quite similar energy contributors to the total interaction energy given by the EDA method. As graphically shown in Figure 3, all the repulsive and attractive contributions (including primary and secondary orbital interactions) are nearly identical which results in the computed rather similar interaction energy between the reactants along the entire transformation for both approaches. This indicates that the deformation energy (ΔE_{strain}) becomes the decisive factor governing the selectivity of this particular Diels−Alder reaction. Indeed, a closer inspection of the ΔE_{strain} curves in Figure 1 clearly indicates that at the transition state region, where the height of the barrier is determined, the exo approach requires a higher deformation, even though the exo transition state **TS1a-exo** is reached earlier. For instance, at the same C···C forming distance of 2.1 Å, a value of ΔE_{strain} = 17.0 kcal/mol was computed for the endo pathway whereas a higher (i.e., more destabilizing) value of ΔE_{strain} = 23.8 kcal/mol was computed for the exo pathway (Figure 2). This can be traced to the fact that, in the exo path, the methyl and TBS groups of the azaborine run into the *N*-methyl and carbonyl groups of the dienophile, therefore increasing the steric hindrance in this particular reaction pathway. A similar behavior was found in the parent textbook Diels−Alder reaction between cyclopentadiene and maleic anhydride[20] which suggests that the deformation energy required to adopt the geometry of the transition state (measured by the ΔE_{strain} term) is the main factor favoring the endo selectivity in these [4 + 2]-cycloaddition reactions.

We also applied the ASM method to understand the activating effect of the $AlCl_3$ catalyst which results in a significant decrease of the activation barrier of the process (see above). According to Figure 4, which shows the ASD for the corresponding preferred endo pathways, once again, a much higher deformation energy is required for the uncatalyzed reaction even though the corresponding transition state **TS-1a-endo′** is reached much earlier than **TS-1a-endo** (computed C···C forming distance of 2.151 Å vs 1.794 Å, respectively, see Figure 1). For instance, at the same C···C distance of 2.3 Å, a value of ΔE_{strain} = 16.3 kcal/mol was computed for the $AlCl_3$-catalyzed reaction whereas a higher value of ΔE_{strain} = 24.4 kcal/mol was computed for uncatalyzed transformation. In addition, the strain energy is not the only factor controlling the rather different activation barriers of these strongly related processes. As seen in Figure 4, the interaction energy (ΔE_{int}) between the deformed reactants is, not surprisingly, much more stabilizing for the catalyzed reaction than for the uncatalyzed one from the very beginning of the cycloaddition. For instance, at the same C···C distance of 2.3 Å, a value of ΔE_{int} = −8.5 kcal/mol was computed for the uncatalyzed cycloaddition whereas a much lower (i.e., more stabilizing) value of ΔE_{int} = −19.0 kcal/mol was computed for the reaction involving the Lewis acid catalyst. Therefore, it can be concluded that the activating effect of $AlCl_3$, resulting in the computed significant decrease of the activation barrier, finds its origin in the combined effect of the lower deformation required by the

DOI: 10.1021/acs.joc.6b01182
J. Org. Chem. 2016, 81, 6554−6562

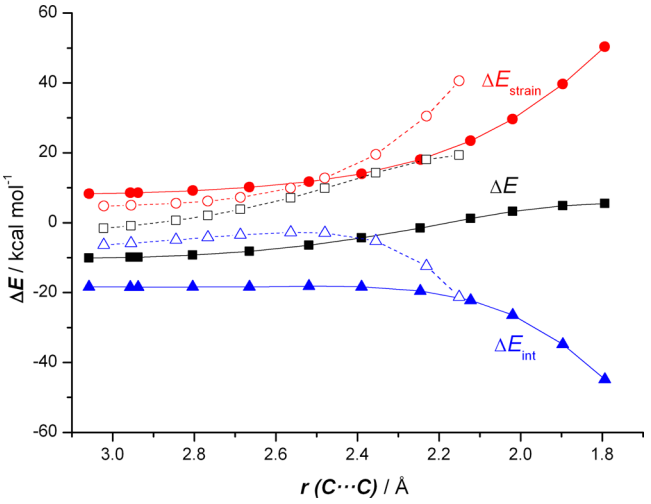

Figure 4. Comparative activation–strain diagrams for the $AlCl_3$-catalyzed (solid lines) and uncatalyzed (dashed lines) Diels–Alder reactions between *N*-methylmaleimide and 1,2-azaborine **1a** along the reaction coordinate projected onto the forming C···C bond distance. All data have been computed at the PCM(toluene)-B3LYP-D3/def2-TZVP//PCM(toluene)-B3LYP-D3/def2-SVP level.

reactants to adopt the geometry of the corresponding transition state and the much stronger interaction between these deformed reactants along the entire reaction coordinate (i.e., up to the transition state).

We next explored the effect of the substituent directly attached to the boron atom in the [4 + 2]-cycloaddition reaction. As commented above, whereas the reaction involving the methyl substituted 1,2-azaborine **1a** proceeds smoothly leading to the corresponding cycloadduct in almost quantitative yield, the reactions involving the hydrogen- and ethynyl-substituted counterparts **1b** and **1c** is severely hampered (reaction yields <5%, see Scheme 1).[11] To understand this remarkable different behavior, the corresponding reaction profiles involving **1a–c** and *N*-methylmaleimide were computed. As depicted in Figure 5, it is confirmed that in all cases the endo approach is kinetically and thermodynamically favored over the exo cycloaddition regardless of the substituent attached to the boron atom. In addition, the computed activation barriers for the favored endo pathways indicate that the Diels–Alder reactivity of **1a** (R = Me) is enhanced as compared to **1b** (R = H) or **1c** (R = ethynyl). Thus, the computed activation barriers (measured from the corresponding reactants) follow the trend **1a** ($\Delta G^{\ddagger}$ = 15.9 kcal/mol) < **1c** ($\Delta G^{\ddagger}$ = 19.1 kcal/mol) < **1b** ($\Delta G^{\ddagger}$ = 20.0 kcal/mol). Despite that, these relatively low activation barriers ($\Delta G^{\ddagger}$ < 20 kcal/mol) together with the computed exothermicity of the processes are not consistent with the observed rather low reaction yields. Therefore, these yields should be ascribed to an

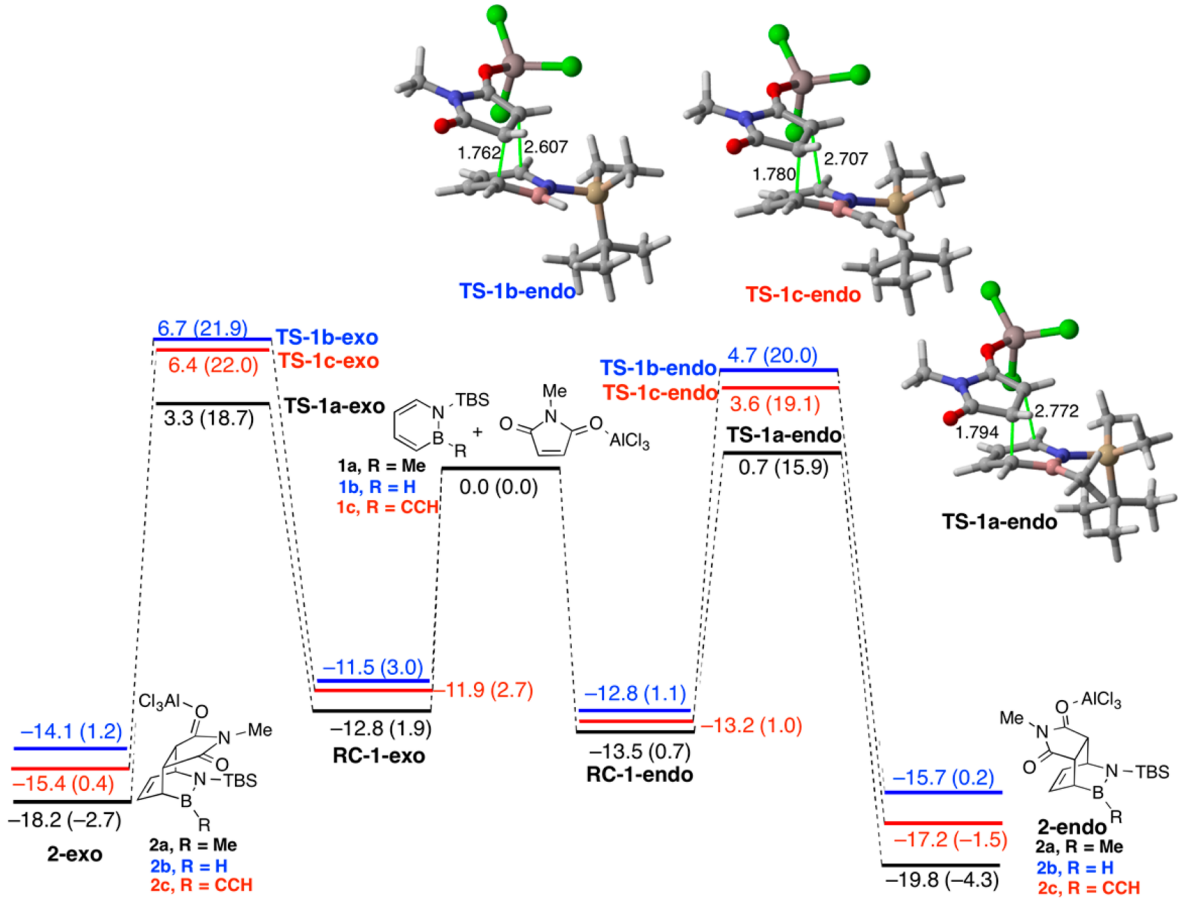

Figure 5. Computed reaction profiles for the Diels–Alder reactions between *N*-methylmaleimide and 1,2-azaborines **1a–c**. Relative energies (ZPVE included) and free energies (computed at 298 K, within parentheses) are given in kcal/mol whereas bond lengths are given in angstroms. All data have been computed at the PCM(toluene)-B3LYP-D3/def2-TZVP//PCM(toluene)-B3LYP-D3/def2-SVP level.

DOI: 10.1021/acs.joc.6b01182
J. Org. Chem. 2016, 81, 6554–6562

experimental issue and not to the intrinsic reactivity of compounds **1b** and **1c**.

The different reactivity of 1,2-azaborines **1a–c** has been suggested to be related to their relative aromaticity strengths.[11] Indeed, our calculations confirm that the computed magnetic aromaticity of these species seems to follow the reactivity trend commented above: **1a** (NICS(0) = −4.1 ppm) < **1c** (NICS(0) = −4.6 ppm) = **1b** (NICS(0) = −4.6 ppm). Moreover, the aromaticity of the corresponding six-membered ring endo transition states also follows this trend: **TS-1a-endo** (NICS(0) = −13.2 ppm) < **TS1c-endo** (NICS(0) = −13.5 ppm) < **TS-1b-endo** (NICS(0) = −14.1 ppm). However, it is highly questionable that such rather low aromaticity differences (less than 1 ppm) become the main factor controlling the Diels–Alder reactivity of these species. In addition, we want to remind the reader that the quantitative use of either isotropic NICS(0) or NICS(1) values has been repeatedly cautioned.[37] For these reasons, we decided to apply the combined ASM–EDA method to understand the influence of the substituent attached to the boron atom on the barrier heights of these Diels–Alder cycloaddition reactions.

To this end, we have compared the favored endo pathways for the [4 + 2]-cycloaddition reactions between *N*-methylmaleimide and **1a** (R = Me) and **1c** (R = ethynyl). From the corresponding ASD in Figure 6, it becomes clear that the

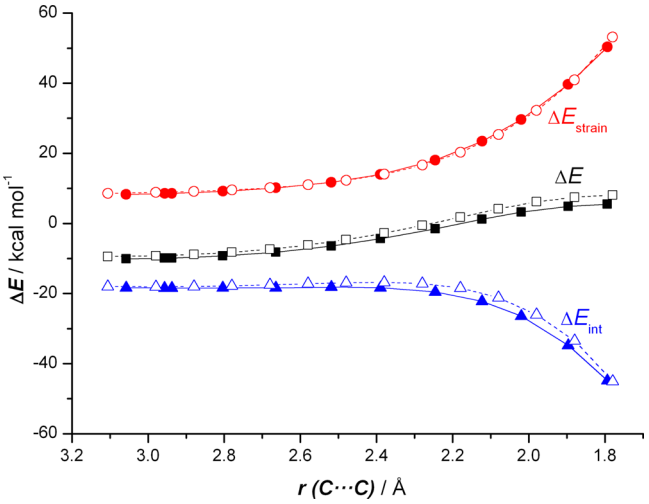

Figure 6. Comparative activation-strain diagrams for the Diels–Alder reactions (endo pathway) between *N*-methylmaleimide and 1,2-azaborine **1a** (solid lines) and 1,2-azaborine **1c** (dashed lines) along the reaction coordinate projected onto the forming C···C bond distance. All data have been computed at the PCM (toluene)-B3LYP-D3/def2-TZVP//PCM(toluene)-B3LYP-D3/def2-SVP level.

required deformation energy (ΔE_{strain}) is nearly identical for both systems from the very beginning of the process up to the transition state region. This indicates that the interaction energy constitutes the sole factor governing the different reactivity of these 1,2-azaborines. Indeed, as shown in Figure 6, the ΔE_{int} term is more stabilizing along the entire reaction coordinate for the process involving **1a** than for that involving **1c** which results in the lower activation energy computed for the former process. Therefore, it can be concluded that the substituent attached to the boron atom only affects the interaction between the 1,2-azaborine and the dienophile.

The EDA method, which further decomposes the interaction energy into its different components, indicates that the higher interaction energy computed for the process involving **1a** is directly related to stronger orbital attractions between the reactants along the reaction coordinate (see Figure S2 in the Supporting Information). The origins of the stronger orbital interactions in the process involving **1a** can be found by using the NOCV (natural orbital for chemical valence) method[38] in combination with the EDA. Thus, the EDA-NOCV approach,[39] which provides pairwise energy contributions for each pair of interacting orbitals to the total bond energy, indicates that, as expected for a normal electronic demand Diels–Alder process, the π(1,2-azaborine) → π^*(*N*-methylmaleimide) molecular orbital interaction dominates the total orbital interactions in these processes. As depicted in Figure 7, which shows the

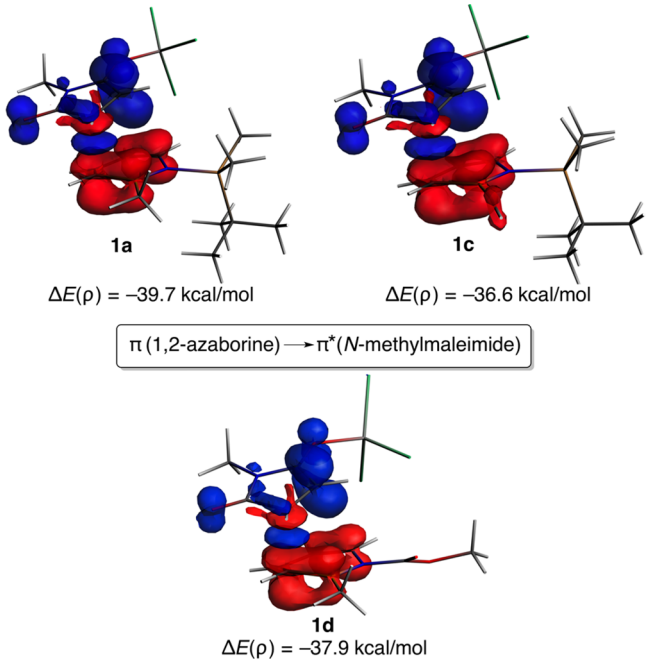

Figure 7. Plot of the deformation densities $\Delta\rho$ of the pairwise orbital interactions between *N*-methylmaleimide and 1,2-azaborines **1a**, **1c** (top) and **1d** (bottom) and associated stabilization energies $\Delta E(\rho)$. The color code of the charge flow is red → blue.

computed NOCV-deformation densities $\Delta\rho$ (charge flow takes place in the direction red → blue), this primary donor/acceptor orbital interaction is clearly stronger in the reaction involving **1a**. Thus, at the same distance of 2.1 Å, the energy associated with this π(diene) → π^*(dienophile) is higher, i.e., more stabilizing, for the reaction involving **1a** than for **1c** (see Figure 7). Therefore, it can be concluded that the stronger orbital interaction in the methyl-substituted 1,2-azaborine **1a**, which results into a stronger interaction along the reaction coordinate, derives mainly from a stronger π(1,2-azaborine) → π^*(*N*-methylmaleimide) molecular orbital interaction.

The influence of the substitution at the nitrogen atom of the 1,2-azaborine was finally addressed. To this end, we compared the N–TBS-substituted species **1a** with the N–CO_2Me counterpart **1d**, a model system of the experimentally used N–Boc azaborine where the *t*Bu group was replaced by a methyl group. As shown in Figure 8, species **1d** is clearly less reactive than **1a** in view of the higher activation barrier computed for the formation of the corresponding endo cycloadduct ($\Delta\Delta G^{\ddagger}_{298}$ = 4.2 kcal/mol). This result is therefore consistent with the much lower reaction yield observed

DOI: 10.1021/acs.joc.6b01182
J. Org. Chem. 2016, 81, 6554–6562

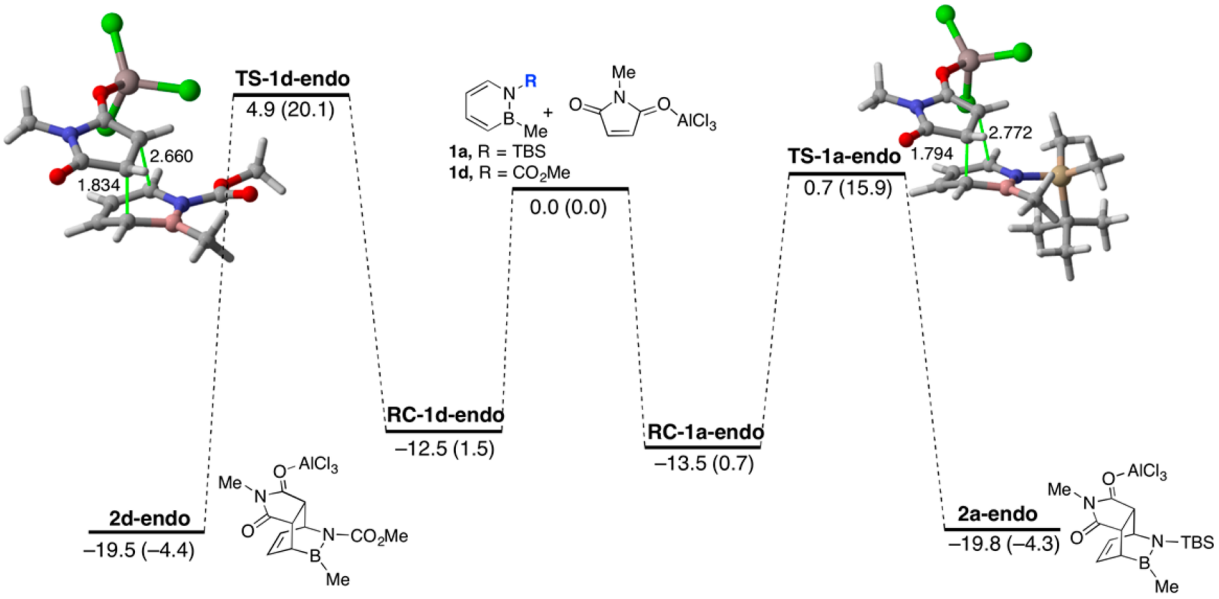

Figure 8. Computed reaction profiles for the Diels–Alder reactions between *N*-methylmaleimide and 1,2-azaborines **1a** and **1d** (endo pathway). Relative energies (ZPVE included) and free energies (computed at 298 K, within parentheses) are given in kcal/mol whereas bond lengths are given in angstroms. All data have been computed at the PCM(toluene)-B3LYP-D3/def2-TZVP//PCM(toluene)-B3LYP-D3/def2-SVP level.

experimentally for the reaction involving the N–Boc derivative (see Scheme 1). Once again, this can be ascribed to the weaker interaction between the deformed reactants as a consequence of the delocalization of the nitrogen lone-pair into the CO_2Me fragment which is reflected into the lower π(1,2-azaborine) → π^*(*N*-methylmaleimide) molecular orbital interaction computed for the reaction involving **1d** ($\Delta E(\rho)$ = −39.7 kcal/mol and −37.9 kcal/mol for **1a** and **1d**, respectively, see Figure 7).

CONCLUSIONS

From the computational study reported herein, the following conclusions can be drawn: (i) the Diels–Alder reaction between *N*-methylmaleide and 1,2-azaborines proceeds concertedly and leads to the corresponding endo cycloadduct. (ii) This selectivity takes place under both kinetic and thermodynamic control and, contrary to the traditional view, is mainly due to the higher deformation energy (measured by the ΔE_{strain} term) required for the exo pathway along the reaction coordinate. (iii) The activating effect of the $AlCl_3$ catalyst, which results in a significant reduction of the activation barrier of the process, finds its origin in the combined effect of the lower deformation required by the reactants to adopt the geometry of the corresponding transition state and the much stronger interaction between these deformed reactants computed for the catalyzed process as compared to the uncatalyzed transformation. (iv) The replacement of the methyl group directly attached to the boron atom of the 1,2-azaborine by either a hydrogen atom or an ethynyl group leads to a remarkable increase of the barrier height of the cycloaddition. A similar effect is found when replacing the TBS group by a CO_2Me substituent at the nitrogen atom of the 1,2-azaborine. (v) Although slightly related to the aromaticity strength of the initial azaborine, this reactivity trend can be ascribed to the different interaction energy (measured by the ΔE_{int} term) between the reactants, which is clearly stronger for the B–methyl/N–TBS derivative. (vi) This is mainly due to stronger orbital interactions as a result of a higher π(1,2-azaborine) → π^*(*N*-methylmaleimide) donor/acceptor interaction in this species as compared to the hydrogen- or ethynyl-substituted and N–CO_2Me counterparts.

ASSOCIATED CONTENT

Supporting Information

The Supporting Information is available free of charge on the ACS Publications website at DOI: 10.1021/acs.joc.6b01182.

Figures S1 and S2, Cartesian coordinates (Å), and total energies (a.u., noncorrected zero-point vibrational energies included) of all the stationary points discussed in the text (PDF)

AUTHOR INFORMATION

Corresponding Author

*E-mail: israel@quim.ucm.es.

Notes

The authors declare no competing financial interest.

ACKNOWLEDGMENTS

Financial support was provided by the Spanish Ministerio de Economía y Competitividad (MINECO) and FEDER (projects CTQ2013-44303-P and CTQ2014-51912-REDC). Y.G.-R. acknowledges the MINECO for a FPI grant.

REFERENCES

(1) Diels, O.; Alder, K. *Justus Liebigs Ann. Chem.* **1928**, *460*, 98.

(2) (a) Fringuelli, F.; Taticchi, A. *The Diels-Alder Reaction: Selected Practical Methods*; John Wiley & Sons, Ltd.: Hoboken, NJ, 2002. See also: (b) Sankararaman, S. *Pericyclic Reactions – A Textbook: Reactions, Applications and Theory*; Wiley: Weinheim, 2005. (c) Kumar, S.; Kumar, V.; Singh, S. P. *Pericyclic Reactions – A Mechanistic and Problem-Solving Approach*; Elsevier: New York, 2015, and references therein.

(3) For recent reviews on the application of Diels–Alder reactions in total synthesis, see: (a) Nicolaou, K. C.; Snyder, S. A.; Montagnon, T.; Vassilikogiannakis, G. *Angew. Chem., Int. Ed.* **2002**, *41*, 1668. (b) Takao, K.-i.; Munakata, R.; Tadano, K.-i. *Chem. Rev.* **2005**, *105*, 4779.

DOI: 10.1021/acs.joc.6b01182
J. Org. Chem. 2016, 81, 6554–6562

(4) For a recent review on the industrial applications of the Diels–Alder reaction, see: Funel, J.-A.; Abele, S. *Angew. Chem., Int. Ed.* **2013**, *52*, 3822.
(5) Alder, K.; Stein, G. *Justus Liebigs Ann. Chem.* **1934**, *514*, 1.
(6) (a) Wassermann, A. *J. Chem. Soc.* **1935**, *825*, 1511. (b) Wassermann, A.; Kistiakowsky, G. B.; Ubbelohde, A. R. *Trans. Faraday Soc.* **1939**, *35*, 841.
(7) Woodward, R. B.; Baer, H. *J. Am. Chem. Soc.* **1944**, *66*, 645.
(8) (a) Ringer, A. L.; Figgs, M. S.; Sinnokrot, M. O.; Sherrill, C. D. *J. Phys. Chem. A* **2006**, *110*, 10822. (b) Maity, S.; Sedlak, R.; Hobza, P.; Patwari, G. N. *Phys. Chem. Chem. Phys.* **2009**, *11*, 9738.
(9) (a) García, J. I.; Mayoral, J. A.; Salvatella, L. *Acc. Chem. Res.* **2000**, *33*, 658. (b) Arrieta, A.; Cossío, F. P.; Lecea, B. *J. Org. Chem.* **2001**, *66*, 6178. (c) Wannere, C. S.; Paul, A.; Herges, R.; Houk, K. N.; Schaefer, H. F., III; Schleyer, P. v. R. *J. Comput. Chem.* **2007**, *28*, 344.
(10) Hoffmann, R.; Woodward, R. B. *J. Am. Chem. Soc.* **1965**, *87*, 4388.
(11) Burford, R. J.; Li, B.; Vasiliu, M.; Dixon, D. A.; Liu, S.-Y. *Angew. Chem., Int. Ed.* **2015**, *54*, 7823.
(12) For selected materials applications of azaborines, see: (a) Liu, A.; Marder, T. *Angew. Chem., Int. Ed.* **2008**, *47*, 242. (b) Lepeltier, M.; Lukoyanova, O.; Jacobson, A.; Jeeva, S.; Perepichka, D. F. *Chem. Commun.* **2010**, *46*, 7007. (c) Marwitz, A. J. V.; Jenkins, J. T.; Zakharov, L. N.; Liu, S.-Y. *Angew. Chem., Int. Ed.* **2010**, *49*, 7444. (d) Abbey, E. R.; Zakharov, L. N.; Liu, S.-Y. *J. Am. Chem. Soc.* **2011**, *133*, 11508. (e) Chrostowska, A.; Xu, S.; Mazière, A.; Boknevitz, K.; Li, B.; Abbey, E. R.; Dargelos, A.; Graciaa, A.; Liu, S.-Y. *J. Am. Chem. Soc.* **2014**, *136*, 11813. (f) Baggett, A. W.; Guo, F.; Li, B.; Liu, S.-Y.; Jäkle, F. *Angew. Chem., Int. Ed.* **2015**, *54*, 11191. (g) Saif, M.; Widom, J. R.; Xu, S.; Abbey, E. R.; Liu, S.-Y.; Marcus, A. H. *J. Phys. Chem. B* **2015**, *119*, 7985.
(13) (a) Liu, L.; Marwitz, A. J. V.; Matthews, B. W.; Liu, S.-Y. *Angew. Chem., Int. Ed.* **2009**, *48*, 6817. (b) Knack, D. H.; Marshall, J. L.; Harlow, G. P.; Dudzik, A.; Szaleniec, M.; Liu, S.-Y.; Heider, J. *Angew. Chem., Int. Ed.* **2013**, *52*, 2599. (c) Kahlert, J.; Austin, C. J. D.; Kassiou, M.; Rendina, L. M. *Aust. J. Chem.* **2013**, *66*, 1118.
(14) For reviews, see: (a) van Zeist, W.-J.; Bickelhaupt, F. M. *Org. Biomol. Chem.* **2010**, *8*, 3118. (b) Fernández, I.; Bickelhaupt, F. M. *Chem. Soc. Rev.* **2014**, *43*, 4953. (c) Fernández, I. *Phys. Chem. Chem. Phys.* **2014**, *16*, 7662. (d) Wolters, L. P.; Bickelhaupt, F. M. *WIREs Comput. Mol. Sci.* **2015**, *5*, 324. See also (e) Fernández, I. In *Discovering the Future of Molecular Sciences*; Pignataro, B., Ed.; Wiley-VCH: Weinheim, 2014; pp 165–187.
(15) (a) von Hopffgarten, M.; Frenking, G. *WIREs Comput. Mol. Sci.* **2012**, *2*, 43. (b) Frenking, G.; Bickelhaupt, F. M. The EDA Perspective of Chemical Bonding. In *The Chemical Bond – Fundamental Aspects of Chemical Bonding*; Frenking, G.; Shaik, S., Eds.; Wiley-VCH: Weinheim, 2014; pp 121–158.
(16) (a) Bento, A. P.; Bickelhaupt, F. M. *J. Org. Chem.* **2007**, *72*, 2201. (b) van Bochove, M. A.; Swart, M.; Bickelhaupt, F. M. *J. Am. Chem. Soc.* **2006**, *128*, 10738. (c) Bento, A. P.; Bickelhaupt, F. M. *J. Org. Chem.* **2008**, *73*, 7290. (d) Fernández, I.; Frenking, G.; Uggerud, E. *Chem. - Eur. J.* **2009**, *15*, 2166. (e) Fernández, I.; Frenking, G.; Uggerud, E. *J. Org. Chem.* **2010**, *75*, 2971. (f) Fernández, I.; Bickelhaupt, F. M.; Uggerud, E. *J. Org. Chem.* **2013**, *78*, 8574. (g) Wolters, L. P.; Ren, Y.; Bickelhaupt, F. M. *ChemistryOpen* **2014**, *3*, 29.
(17) (a) Fernández, I.; Bickelhaupt, F. M.; Cossío, F. P. *Chem. - Eur. J.* **2009**, *15*, 13022. (b) Fernández, I.; Cossío, F. P.; Bickelhaupt, F. M. *J. Org. Chem.* **2011**, *76*, 2310. (c) Nieto Faza, O.; Silva López, C.; Fernández, I. *J. Org. Chem.* **2013**, *78*, 5669. (d) Fernández, I.; Bickelhaupt, F. M.; Cossío, F. P. *Chem. - Eur. J.* **2012**, *18*, 12395. (e) Hong, X.; Liang, Y.; Houk, K. N. *J. Am. Chem. Soc.* **2014**, *136*, 2017. (f) Fernández, I.; Bickelhaupt, F. M.; Cossío, F. P. *Chem. - Eur. J.* **2014**, *20*, 10791. (g) Fernández, I.; Cossío, F. P. *J. Comput. Chem.* **2016**, *37*, 1265 (see also ref 32).
(18) (a) van Zeist, W.-J.; Bickelhaupt, F. M. *Dalton Trans.* **2011**, *40*, 3028. and references therein. (b) Wolters, L. P.; Bickelhaupt, F. M. *ChemistryOpen* **2013**, *2*, 106. (c) Green, A. G.; Liu, P.; Merlic, C. A.; Houk, K. N. *J. Am. Chem. Soc.* **2014**, *136*, 4575. (d) Fernández, I.; Wolters, L. P.; Bickelhaupt, F. M. *J. Comput. Chem.* **2014**, *35*, 2140. (e) Sosa Carrizo, E. D.; Bickelhaupt, F. M.; Fernández, I. *Chem. - Eur. J.* **2015**, *21*, 14362.
(19) (a) Fernández, I.; Solà, M.; Bickelhaupt, F. M. *Chem. - Eur. J.* **2013**, *19*, 7416. (b) Fernández, I.; Solà, M.; Bickelhaupt, F. M. *J. Chem. Theory Comput.* **2014**, *10*, 3853. (c) Bickelhaupt, F. M.; Solà, M.; Fernández, I. *Chem. - Eur. J.* **2015**, *21*, 5760. (d) García-Rodeja, Y.; Solà, M.; Bickelhaupt, F. M.; Fernández, I. *Chem. - Eur. J.* **2016**, *22*, 1368.
(20) Fernández, I.; Bickelhaupt, F. M. *J. Comput. Chem.* **2014**, *35*, 371.
(21) Frisch, M. J.; Trucks, G. W.; Schlegel, H. B.; Scuseria, G. E.; Robb, M. A.; Cheeseman, J. R.; Scalmani, G.; Barone, V.; Mennucci, B.; Petersson, G. A.; Nakatsuji, H.; Caricato, M.; Li, X.; Hratchian, H. P.; Izmaylov, A. F.; Bloino, J.; Zheng, G.; Sonnenberg, J. L.; Hada, M.; Ehara, M.; Toyota, K.; Fukuda, R.; Hasegawa, J.; Ishida, M.; Nakajima, T.; Honda, Y.; Kitao, O.; Nakai, H.; Vreven, T.; Montgomery, J. A., Jr.; Peralta, J. E.; Ogliaro, F.; Bearpark, M.; Heyd, J. J.; Brothers, E.; Kudin, K. N.; Staroverov, V. N.; Kobayashi, R.; Normand, J.; Raghavachari, K.; Rendell, A.; Burant, J. C.; Iyengar, S. S.; Tomasi, J.; Cossi, M.; Rega, N.; Millam, J. M.; Klene, M.; Knox, J. E.; Cross, J. B.; Bakken, V.; Adamo, C.; Jaramillo, J.; Gomperts, R.; Stratmann, R. E.; Yazyev, O.; Austin, A. J.; Cammi, R.; Pomelli, C.; Ochterski, J. W.; Martin, R. L.; Morokuma, K.; Zakrzewski, V. G.; Voth, G. A.; Salvador, P.; Dannenberg, J. J.; Dapprich, S.; Daniels, A. D.; Farkas, Ö.; Foresman, J. B.; Ortiz, J. V.; Cioslowski, J.; Fox, D. J. *Gaussian 09, Revision D.01*; Gaussian, Inc., Wallingford, CT, 2009.
(22) (a) Becke, A. D. *J. Chem. Phys.* **1993**, *98*, 5648. (b) Lee, C.; Yang, W.; Parr, R. G. *Phys. Rev. B: Condens. Matter Mater. Phys.* **1988**, *37*, 785. (c) Vosko, S. H.; Wilk, L.; Nusair, M. *Can. J. Phys.* **1980**, *58*, 1200.
(23) Grimme, S.; Antony, J.; Ehrlich, S.; Krieg, H. *J. Chem. Phys.* **2010**, *132*, 154104.
(24) Weigend, F.; Ahlrichs, R. *Phys. Chem. Chem. Phys.* **2005**, *7*, 3297.
(25) (a) Miertuš, S.; Scrocco, E.; Tomasi, J. *Chem. Phys.* **1981**, *55*, 117. (b) Pascual-Ahuir, J. L.; Silla, E.; Tuñón, I. *J. Comput. Chem.* **1994**, *15*, 1127. (c) Barone, V.; Cossi, M. *J. Phys. Chem. A* **1998**, *102*, 1995.
(26) McIver, J. W.; Komornicki, A. K. *J. Am. Chem. Soc.* **1972**, *94*, 2625.
(27) González, C.; Schlegel, H. B. *J. Phys. Chem.* **1990**, *94*, 5523.
(28) Chen, Z.; Wannere, C. S.; Corminboeuf, C.; Puchta, R.; Schleyer, P. v. R. *Chem. Rev.* **2005**, *105*, 3842.
(29) Bader, R. F. W. *Atoms in Molecules - A Quantum Theory*; Clarendon Press: Oxford, 1990.
(30) For related examples on the aromaticity of transition structures, see: Schleyer, P. v. R.; Wu, J. I.; Cossío, F. P.; Fernández, I. *Chem. Soc. Rev.* **2014**, *43*, 4909.
(31) Wolinski, K.; Hinton, J. F.; Pulay, P. *J. Am. Chem. Soc.* **1990**, *112*, 8251.
(32) (a) Ess, D. H.; Houk, K. N. *J. Am. Chem. Soc.* **2007**, *129*, 10646. (b) Ess, D. H.; Houk, K. N. *J. Am. Chem. Soc.* **2008**, *130*, 10187. (c) Ess, D. H.; Jones, G. O.; Houk, K. N. *Org. Lett.* **2008**, *10*, 1633. For relevant studies on other pericyclic reactions by Houk's group, see: (d) Schoenebeck, F.; Ess, D. H.; Jones, G. O.; Houk, K. N. *J. Am. Chem. Soc.* **2009**, *131*, 8121. (e) Xu, L.; Doubleday, C. E.; Houk, K. N. *J. Am. Chem. Soc.* **2010**, *132*, 3029. (f) Krenske, E. H.; Houk, K. N.; Holmes, A. B.; Thompson, J. *Tetrahedron Lett.* **2011**, *52*, 2181.
(33) Becke, A. D. *Phys. Rev. A: At., Mol., Opt. Phys.* **1988**, *38*, 3098. (b) Perdew, J. P. *Phys. Rev. B: Condens. Matter Mater. Phys.* **1986**, *33*, 8822.
(34) (a) Snijders, J. G.; Baerends, E. J.; Vernoojs, P. *At. Data Nucl. Data Tables* **1981**, *26*, 483. (b) Krijn, J.; Baerends, E. J. *Fit Functions in the HFS-Method*; Internal Report (in Dutch); Vrije Universiteit Amsterdam: The Netherlands, 1984.
(35) ADF, SCM, *Theoretical Chemistry*; Vrije Universiteit: Amsterdam, The Netherlands, http://www.scm.com.

DOI: 10.1021/acs.joc.6b01182
J. Org. Chem. 2016, 81, 6554–6562

(36) The alternative stepwise mechanism has been also considered. However, the corresponding transition state associated with the formation of only one C−C bond lies 10.4 kcal/mol above the concerted transition state **TS-1a-endo**. In addition, the corresponding zwitterionic intermediate is also highly destabilized (it lies 10.2 kcal/mol above **TS-1a-endo**). No other stepwise pathways (i.e., diradical pathway) could be located. Therefore, the alternative stepwise mechanism can be safely ruled out.
(37) (a) Gomes, J. A. N. F.; Mallion, R. B. *Chem. Rev.* **2001**, *101*, 1349. (b) Katritzky, A. R.; Jug, K.; Oniciu, D. C. *Chem. Rev.* **2001**, *101*, 1421. (c) Poater, J.; Duran, M.; Solà, M.; Silvi, B. *Chem. Rev.* **2005**, *105*, 3911.
(38) Mitoraj, M.; Michalak, A. *J. Mol. Model.* **2007**, *13*, 347.
(39) Mitoraj, M. P.; Michalak, A.; Ziegler, T. *J. Chem. Theory Comput.* **2009**, *5*, 962.

DOI: 10.1021/acs.joc.6b01182
J. Org. Chem. 2016, 81, 6554−6562